



Linking the kinds of bulges with types of arms structures in disks

S. dos Anjos and M. B. da Silva

Universidade de São Paulo, Departamento de Astronomia, Rua do Matão, 1226, São Paulo, Brasil, e-mail: sandra@astro.iag.usp.br

Abstract. From a sample of late-type non-barred spiral galaxies, with different types of arms structures - grand design, flocculent and multiple, we conducted a study in order to verify if classical bulges and pseudobulges are components found in different kinds of arms structure in disks, following predictions from Secular Evolution Scenario (SES) numerical simulations. Images in four passband from SDSS were used in order to apply the 2D-BUDDA Code to obtain photometric and structural parameters. From those parameters we built several residual images of bulges, disks and totals. Colors and radial brightness profiles were also performed. We have developed a method to classify arms and bulges from the residual images and we have used also the behaviors of colors and brightness profiles. We have verified that 62% of the sample are suggestive of have pseudobulges (24% pure pseudobulges and 38% classical bulges coexisting with pseudobulges (CB+PB)), 33% have classical bulges and approximately 5% of the galaxies are bulgeless. Our results also indicate that there exist a tendency that galaxies that have pure pseudobulges also have DA or MA arms and are bluer. Galaxies with classical bulges and pseudobulges coexisting have DA or MA arms and median blue color when compared with those that pure pseudobulges. Classical bulges have larger amplitude of arms patterns, including 2A(58%), MA(14%), DA(14%) and no arms defined(14%). These results could be relevant in order to understand the formation, evolution and the dynamic of galaxies.

Key words. Galaxies: bulges, pseudobulges, discs – Galaxy: formation, evolution – Galaxy: secular evolution

1. Introduction

Several observational studies during the last 3 decades are showing that the monolithic and/or hierarchical scenarios of formation and evolution of galaxies cannot explain alone all observed properties in galaxies. The amplitude of the morphological types, the trichotomy in the observed general properties of the bulges (classical, box-shaped, pseudobulge), the presence of massive and recent stellar formation

observed by Hubble Space Telescope in some bulges, besides of the expressive rotation observed in some of them when compared with the classical ones, in particular, the cylindrical rotations, are some examples of these diversities. Another great surprise is that the bulgeless galaxies are not also so rare as we thought (Kormendy et al. 2010), challenging our picture of galaxy formation by hierarchical clustering. The Secular Evolution Scenario (SES) has emerged as a new paradigm to complement the monolithic and hierarchical scenarios, and

Send offprint requests to: S. dos Anjos

could explain some of the observed properties cited above.

The main driver of Secular Evolution in disk galaxies is the presence of global instabilities such as bars, spiral arms, oval disks and bending instabilities and may play an important role in evolution of disk galaxies. These instabilities change the mass and angular momentum distribution of the disk provoking a slow dynamical and structural evolution of galaxy. As the nature of grand-design arms seems different from those in flocculent galaxies we will explore in this work some predictions from SES, verifying whether different kinds of bulges are living in different structures of arms in disks.

2. Sample and photometric bulge-disk decomposition

From (Elmegreen & Elmegreen 1982); (Elmegreen & Elmegreen 1987) Catalogues we have selected 21 galaxies according to the arms structure. In order to proceed with the photometric studies and also to obtain the colors (u-g), (g-r), (r-z) profiles, images in 4 passband (u, g, r and z) were selected from SDSS database. In this work we will present the results for six of them as can be seen in Table 1 and Figure 1. A full version of this work including all 21 galaxies analysed in this study will be available in dosanjos 2013.

2.1. Photometric decomposition - 2D BUDDA CODE

We have applied for all sample and in the 4 passband (u, g, r, z) the corrections of extinction effects using the data from SDSS. For internal absorption we have used the (Tully et al. 1998) work. We have also done the sky correction, elimination of spurious pixels, removal of stars, foreground and background galaxies, besides of the calibration of the images. Next step was to perform a two-dimensional bulge-disk decomposition applying the BUDDA code. In this code the algorithm design an image of galaxies composed by just two major compo-

nents: bulge and the disk. For the disk we have adopted an exponential light distribution

$$I_d(r) = I_{0d}e^{-r/h} \quad (1)$$

where h is the disk scale length, I_{0d} represents the central brightness, and r is the semi-major axis of the elliptical isophotes having ellipticity e_d . Both components, the bulge and the disk, share a common center located at x_0, y_0 , but the ellipticity (e_d, e_b) and the position angle (PA_d, PA_b) are not necessarily equal. We fitted the bulge profile using the Sérsic luminosity profile

$$I_{b(r)} = I_{0b}10^{-b_n[(r/r_{eb})^{1/n}]} \quad (2)$$

where r_{eb} is the effective radius, I_{0b} is the central brightness, and n is an index that controls the shape of the brightness profile. For $n=4$, we recover the de Vaucouleurs profile, while for $n=1$ we have an exponential profile.

Therefore, the index n is an important quantity describing the radial variations of the brightness profile. The numerical constant b_n is defined in such a way that the effective radius, r_{eb} , contains half of the total bulge luminosity and its value is approximately given by $b_n \approx 0.868n + 0.142$. At $r = r_{eb}$, $I_b = I_{eb}$, the bulge effective surface brightness. The coordinate r indicates the semimajor axis of the bulge elliptical isophotes centered on x_0, y_0 , having an ellipticity e_b and a position angle PA_b . The code includes correction of seeing and also a supplementary correction of the sky. For a complete description of BUDDA, please refer to de (deSouza, Gadotti & dos Anjos 2004).

3. Results

From the Code we have obtained photometric and structural parameters and we built several synthetic and residual images. We have noticed that color ranges from color profiles, the type of residual arms structure besides bulge brightness profile contribution could be categorized and synthesized as following:

A2– Two arms clearly coming out from the central region of galaxy similar to the grand-design spirals; central brightness profile between $2.0 < (u - g) < 2.5$; small contribution of the bulge brightness profile.

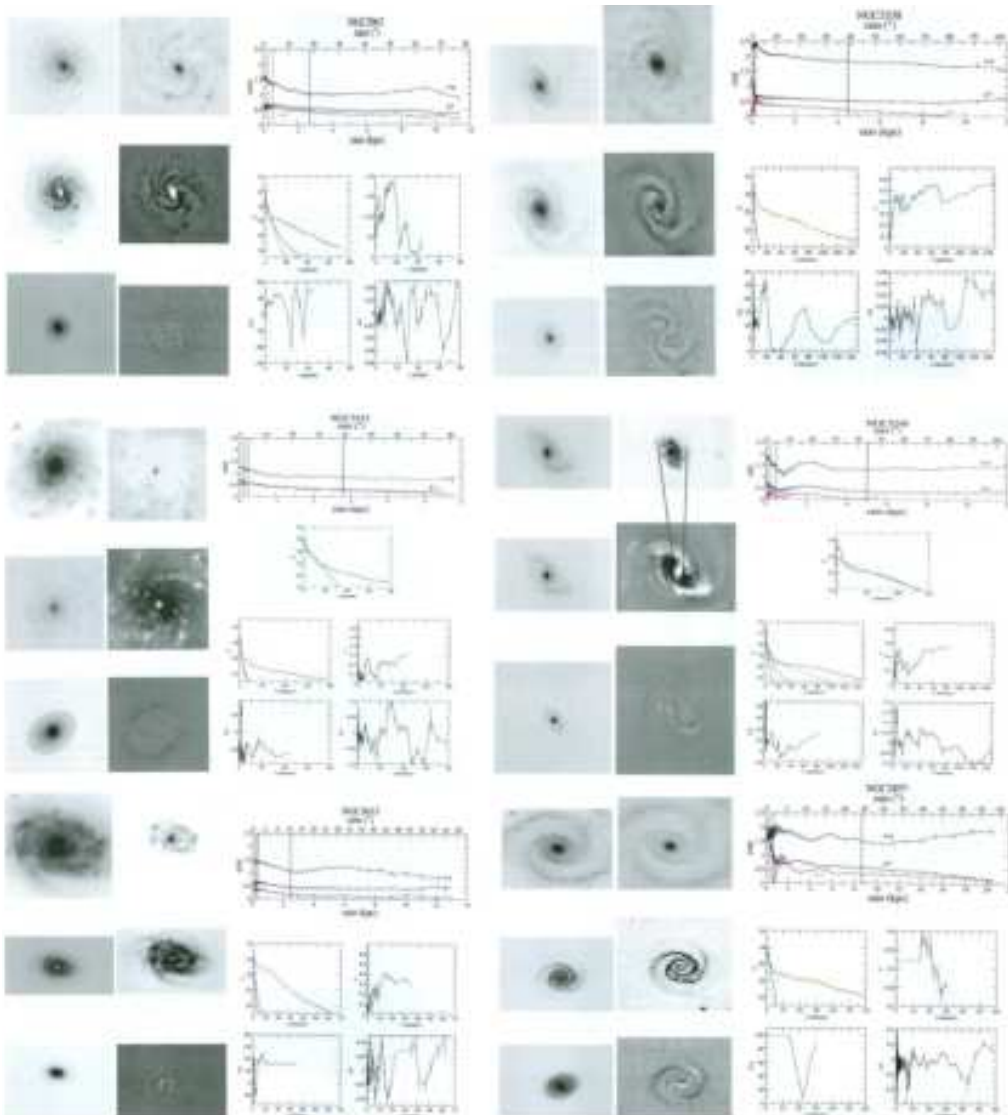


Fig. 1. Images (r-band): left to right, top to bottom; 1) original; 2) bulge's residual; 3) disk's residual; 4) total residual; 5) model from IRAF-BMODEL (z-band); 6) total residual (z-band).

Plots: upper panels show the color profile behavior - vertical lines show the limit of seeing effects (black), the characteristic length of disk's (blue) and bulge's (red); others panels, show brightness profile fitting and geometric parameters behavior. The reader can observe the classification of arms (A2, AD or AM) and identification of bulges (CB, PB or CB/PB) in Table 1.

AD– Diffuse arms clearly coming out from the central region of galaxy; central brightness profile between $1.5 < (u - g) < 2.0$; and relatively medium contribution of bulge brightness profile.

AM– Multiple and chaotic arms, spread out in the whole disk, with clear HII regions scattered throughout the length of the disk; central brightness profile between $1.0 < (u -$

Table 1. Grand-design (GD), Flocculent (FL) and Multi-arms (MA) Galaxies. Column (1): NGC identifier and class of arms of Elmegreen (EC); column (2): Hubble types and errors; column (3) and (4) axial ratio at 25mag arcsec^{-2} and apparent magnitude in B band and errors; **columns (5) and (6):** arms (AM-multi-arms; AD-diffuse arms; A2-2 arms) and bulges (CB-classical; PB-pseudobulges; CB/PB-classical and pseudobulges coexisting) classes obtained from this work

Name - (EC)	Type (T) (error)	R_{25} (error)	B (mag) (error)	AC	BC
NGC2857 - GD	5.0(0.3)	0.05(0.05)	13.80(0.30)	A2	CB
NGC2967 - GD	5.0(0.3)	0.04(0.03)	11.91(0.15)	AM	CB/PB
NGC3338 - GD	5.0(0.3)	0.21(0.02)	11.41(0.18)	A2	CB
NGC3423 - FC	6.0(0.3)	0.07(0.02)	11.54(0.16)	AM	PB
NGC5248 - GD	4.0(0.3)	0.14(0.02)	10.64(0.17)	A2	CB/PB
NGC5633 - MA	3.0(0.4)	0.21(0.03)	12.83(0.15)	AD	PB

$g) < 1.5$; none or little contribution from the bulge brightness profile.

From the residual images of the bulges, we could check if the central parts of galaxies show structures as a classical bulge (CB), or substructures, as those provided by Secular Evolution Scenarios, named pseudobulges (PB) or the coexistence of both (CB/PB). We identified 62% as having pseudobulges: 38% classical bulges coexisting with pseudobulges (BC + CP) and 24% pure pseudobulges. As pure classical bulges we found 33%. We have also found that almost 5% are bulgeless. We have verified that galaxies that have pure pseudobulges also have DA or MA arms and are bluer. Galaxies with classical bulges and pseudobulges coexisting have DA or MA arms and median blue color when compared with those that pure pseudobulges. Classical bulges have larger amplitude of arms patterns, including the classes 2A(58%), MA(14%), DA(14%) and no arms defined(14%).

4. Conclusion

The analysis has revealed an enormous diversity of substructures immersed in the dim

light of the original images on both disks and bulges components. The total residual images of galaxies besides those of bulge and disk components were crucial to observed the detailed structures of these components. Our results indicate a tendency that galaxies that have pure pseudobulges (PB) also have AD or AM arms and are the bluest of the sample. Galaxies with coexisting classical bulges and pseudobulges (CB+PB) also have AD or AM arms, and median blue color when compared with those that have pure pseudobulges. Classical bulges have a larger amplitude of arms patterns, including A2, AM and AD.

References

- de Souza, R. E., Gadotti, D. A., dos Anjos, S. 2004, ApJS, 153, 411
dos Anjos, S., da Silva, M. B. 2012, (in prep.)
Elmegreen, D. M. & Elmegreen, B. G. 1982, MNRAS, 201, 1021
Elmegreen, D. M. & Elmegreen, B. G. 1987, ApJ, 314, 3
Kormendy, J., Drory, N., Bender, R., & Cornell, M. E. 2010, ApJ, 723, 54
Tully, R. B., et al., 1998, AJ, 115, 2264